

The Reactive Chemisorption of Alkyl Iodides at Cu(110) and Ag(111) Surfaces: A Combined STM and XPS Study

James Bushell, Albert F. Carley, Mark Coughlin, Philip R. Davies,* Dyfan Edwards, David J. Morgan, and Martin Parsons

School of Chemistry, Main Building, Cardiff University, Cardiff CF10 3AT, UK

Received: March 15, 2005

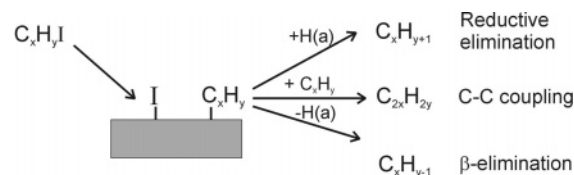
The chemisorption of methyl and phenyl iodide has been studied at Cu(110) and Ag(111) surfaces at 290 K with STM and XPS. At both surfaces dissociative adsorption of both molecules leads to chemisorbed iodine, with the STM showing $c(2 \times 2)$ and $(\sqrt{3} \times \sqrt{3})R30$ structures at the Cu(110) and Ag(111) surfaces, respectively. At the Cu(110) surface a comparison of coexisting $c(2 \times 2)$ I(a) and $p(2 \times 1)$ O(a) domains shows the iodine adatoms to be chemisorbed in hollow sites with evidence at low coverage for diffusion in the $\langle 1\bar{1}0 \rangle$ direction. In the case of methyl iodide no carbon adsorption is observed at either the silver or the copper surfaces, but chemisorbed phenyl groups are imaged at the Cu(110) surface after exposure to phenyl iodide. The STM images show the phenyl groups as bright features approximately 0.7 nm in diameter and 0.11 nm above the iodine adlayer, reaching a maximum surface concentration after ~ 6 Langmuir exposure. However, the phenyl coverage decreases with subsequent exposures to PhI and is negligible by ~ 1000 L exposure, consistent with the formation and desorption of biphenyl. The adsorbed phenyls are located above hollow sites in the substrate, they are stabilized at the top and bottom of step edges and in paired chains (1.1 nm apart) on the terraces with a regular interphenyl spacing within the chains of 1.0 nm in the $\langle 1\bar{1}0 \rangle$ direction. The interphenyl ring spacing and diffusion of *individual* phenyls from within the chains shows that the chains do not consist of biphenyl species but may be a precursor to their formation. Although the XPS data shows carbon present at the Ag(111) surface after exposure to PhI, no features attributable to phenyl groups were observed by STM.

Introduction

Alkyl iodides dissociate readily below room temperature at most atomically clean metal surfaces yielding chemisorbed iodine and an adsorbed alkyl group. The latter can undergo a number of different processes including C–C coupling and hydride elimination, resulting in a hydrocarbon that desorbs; some of the observed steps are illustrated in Scheme 1.

Understanding the pathways followed by the alkyl fragments is relevant to many industrially important metal catalyzed reactions including hydrogenation, dehydrogenation, reforming, Fischer–Tropsch and the catalytic decomposition of alkyl halide pollutants. The complexity of heterogeneous catalysts prevents a close examination of the individual steps, but at single crystal surfaces intermediates can be isolated and studied in detail. This approach has been adopted by several researchers, notably Bent and co-workers,^{1,2} and a number of alkyl halides have been studied, principally by thermal desorption, vibrational spectroscopy, and NEXAFS.^{2–14} Considerable progress has been made in delineating the reaction pathways available to alkyl fragments at different surfaces, and attention must now switch to the factors affecting the selectivity of one path over another. An important contribution to this selectivity will be the local environment and in particular the local structure and surface concentration. Until recently, the ability to probe the local environment of the adsorbed alkyl groups has been lacking, but the advent of proximal probe methods provides an opportunity to address this issue and also reexamine many of the conclusions reached in previous studies.

SCHEME 1: Some of the Reaction Pathways Available to Alkyl Fragments at Metal Surfaces



The present approach combines STM with quantitative XPS and allows the study of local surface structure, including adsorbate mobility, as a function of surface concentration. Methyl iodide, the simplest and most reactive of the alkyl halides, is compared with phenyl iodide, which gives rise to a larger adsorbate for which surface structure may play a more important role. The two adsorbates have been studied at two surfaces: Cu(110), on which alkyl halide adsorption has been studied in detail by thermal desorption,^{6,11,15,16} and Ag(111), which has been less extensively investigated.

Experimental Section

Experiments were conducted using a combined variable temperature STM/XPS instrument (Omicron Vacuum Physik) equipped with a dual aluminum and magnesium K α photon source. Except where stated otherwise, spectra were recorded with a pass energy of 50 eV, resulting in typical peak half-widths of c.a. 1.8 eV. Spectra were obtained by the combination of 10–20 individual scans over a 25 eV wide region, with a total acquisition time of between 10 min (O(1s), I(3d), and Cu

* Corresponding author. E-mail: daviespr@cf.ac.uk

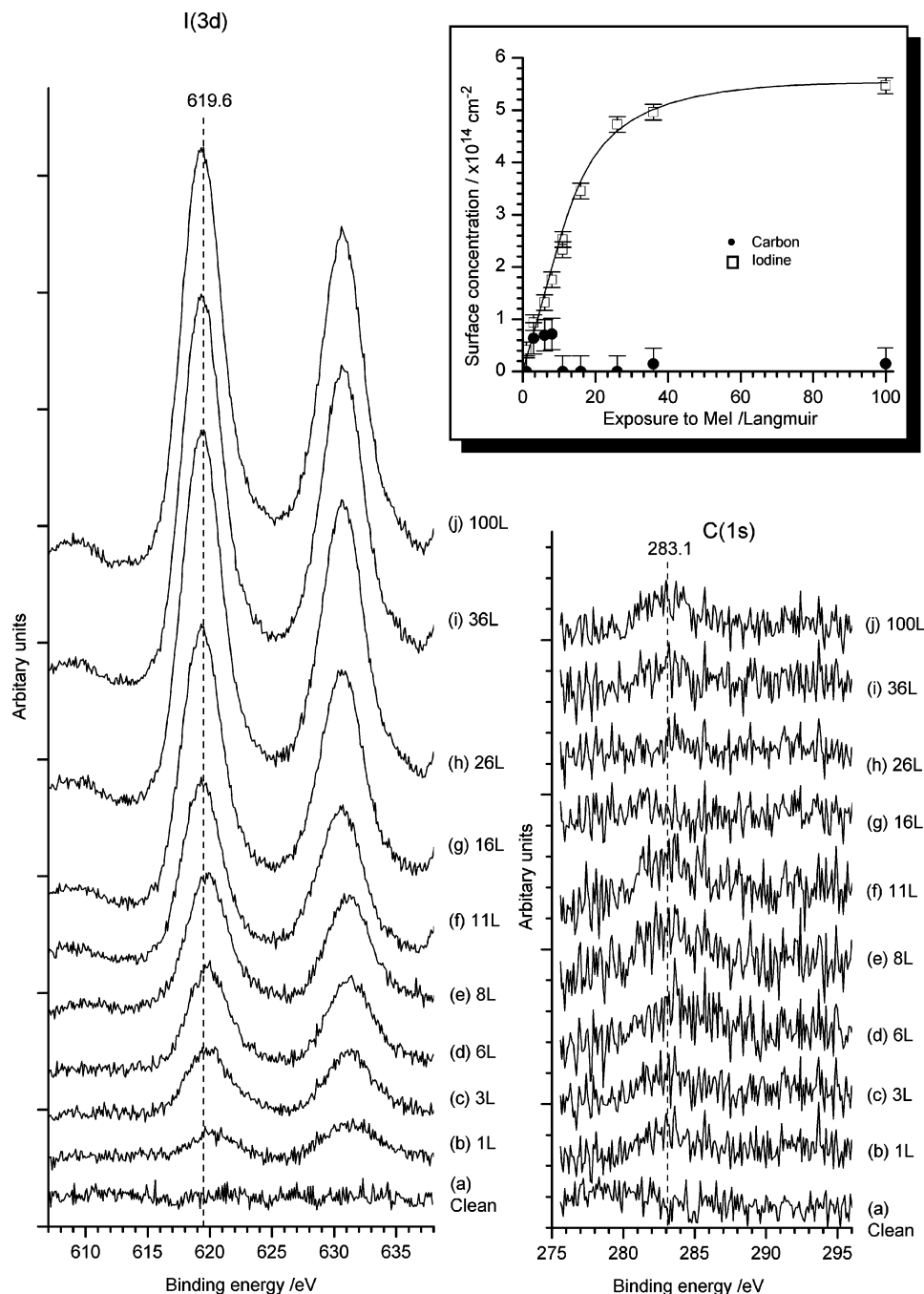


Figure 1. I(3d) and C(1s) XPS spectra of the dissociative chemisorption of methyl iodide at a clean Cu(110) surface at 290 K. Exposures to MeI are given on the figure. Inset: the surface concentration of iodine and carbon calculated from the XP spectra plotted as a function of exposure to MeI. The solid line is to guide the eye.

(2p) spectra) to 20 min (C(1s) spectra). The spectra were calibrated to the clean Cu(2p_{3/2}) peak at 932.7 eV. XPS data were acquired using commercial software (Spectra, Ron Unwin) and analyzed using software developed in-house. Surface concentrations were calculated from XP peak areas using a method discussed previously.^{17,18} We estimate the error in the surface concentrations of oxygen and iodine to be $\pm 1.5 \times 10^{13} \text{ cm}^{-2}$, and slightly greater in the case of carbon, which has a weaker signal. STM tunneling conditions, (i.e., sample bias (V_s) and tunneling current (I_T)), are given in the figure legends. STM images were analyzed using WSxM.¹⁹

The dimensions of the sample were 7 mm by 7 mm with a thickness of approximately 0.5 mm; it was orientated to within 0.5 degrees of the (110) plane and polished mechanically down to 0.25 mm. Cleaning involved cycles of Ar⁺ sputtering (0.65

keV, 20 $\mu\text{A cm}^{-2}$ for 10 min) and annealing for 40 min at 700 K. This resulted in flat terraces approximately 10–20 nm wide in the STM images. Sample cleanliness was checked by XPS. Gases were dosed via a leak valve at pressures of between 10^{-9} to 5×10^{-7} mbar. The phenyl iodide and methyl iodide (Aldrich, 99.5%) were subjected to several freeze-pump-thaw cycles using a dry ice/acetone slush and monitored with in situ mass spectrometry during dosing. Oxygen (Argo Ltd, 99.998%) was used as received.

Results

Methyl Iodide Adsorption at Cu(110) Surfaces. In Figure 1, the chemisorption of methyl iodide (MeI) at a Cu(110) surface at 290 K is followed by XPS. Two peaks, assigned to I(3d_{5/2})

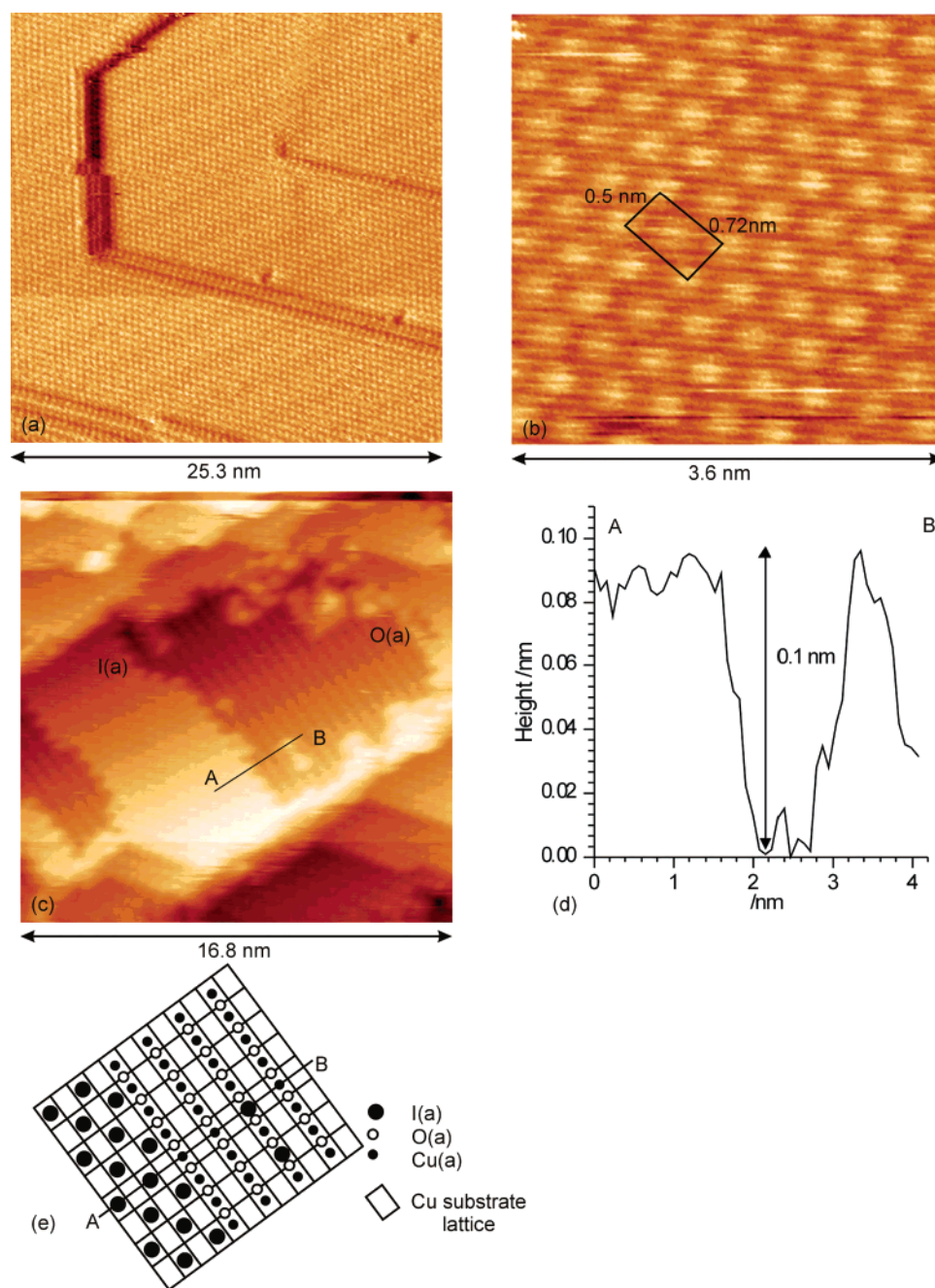


Figure 2. STM images of the iodine adlayer formed at Cu(110) surfaces by the dissociative adsorption of methyl iodide at 290 K. (a) Adsorption at a clean surface $\sigma_I = 5.5 \times 10^{14} \text{ cm}^{-2}$ (calculated from the corresponding XP spectra). $V_S = -1.41 \text{ V}$, $I_T = 1.93 \text{ nA}$. (b) Close-up of $c(2 \times 2)I(a)$ adlayer, $V_S = -1.07 \text{ V}$, $I_T = 3.53 \text{ nA}$. (c) Adsorption at a partially oxidized surface, $\sigma_O = 1.0 \times 10^{14} \text{ cm}^{-2}$. $V_S = -1.03 \text{ V}$, $I_T = 3.47 \text{ nA}$. (d) Line profile over AB. (e) Model of the coexisting $p(2 \times 1)O(a)$ and $c(2 \times 2)I(a)$ lattices showing the position of the iodine adatoms relative to the oxygens.

and $I(3d_{3/2})$, develop in the $I(3d)$ region with binding energies of 619.6 and 630.9 eV respectively, characteristic of chemisorbed iodine. However, only a negligible concentration of carbon is present in the $C(1s)$ spectrum, implying dissociation of the C–I bond and desorption of C_xH_y . Inset in Figure 1 is a plot of the surface concentration of iodine and carbon (calculated from the XP peak areas) as a function of exposure; saturation of the iodine adlayer occurs at $5.5 \times 10^{14} \text{ cm}^{-2}$ after an exposure of $\sim 80 \text{ L}$ (1 L = 1 Langmuir = 10^{-6} Torr s).

The STM images in Figures 2a,b are of a Cu(110) surface exposed to 72 L of MeI and show the iodine adlayer to be characterized by a $c(2 \times 2)$ unit cell, consistent with the iodine concentration ($\sigma_I = 5.5 \times 10^{14} \text{ cm}^{-2}$, $\theta_I = 0.5$) calculated from the corresponding XP spectra. The iodine lattice is very uniform

with few defects and no grain boundaries, suggesting a significant degree of mobility as it develops. Figure 2c shows an STM image of islands of $c(2 \times 2)I(a)$ coexisting with $p(2 \times 1)O(a)$ structures, formed by exposing a partially oxidized Cu(110) surface ($\sigma_O = 1.4 \times 10^{14} \text{ cm}^{-2}$) to MeI at 290 K. STM images were acquired during the exposure, and the $c(2 \times 2)I$ adlayer was observed to develop on the areas of clean copper between oxygen islands without disturbing either the oxygen lattice or the nearby step edges.

The $c(2 \times 2)I(a)$ and $p(2 \times 1)O(a)$ structures in Figure 2c share a single terrace, and the apparent height profile over the surface (Figure 2d) shows a difference of approximately 0.1 nm between the iodine and the oxygen lattice. More detailed analysis of the STM images shows that the maxima of the

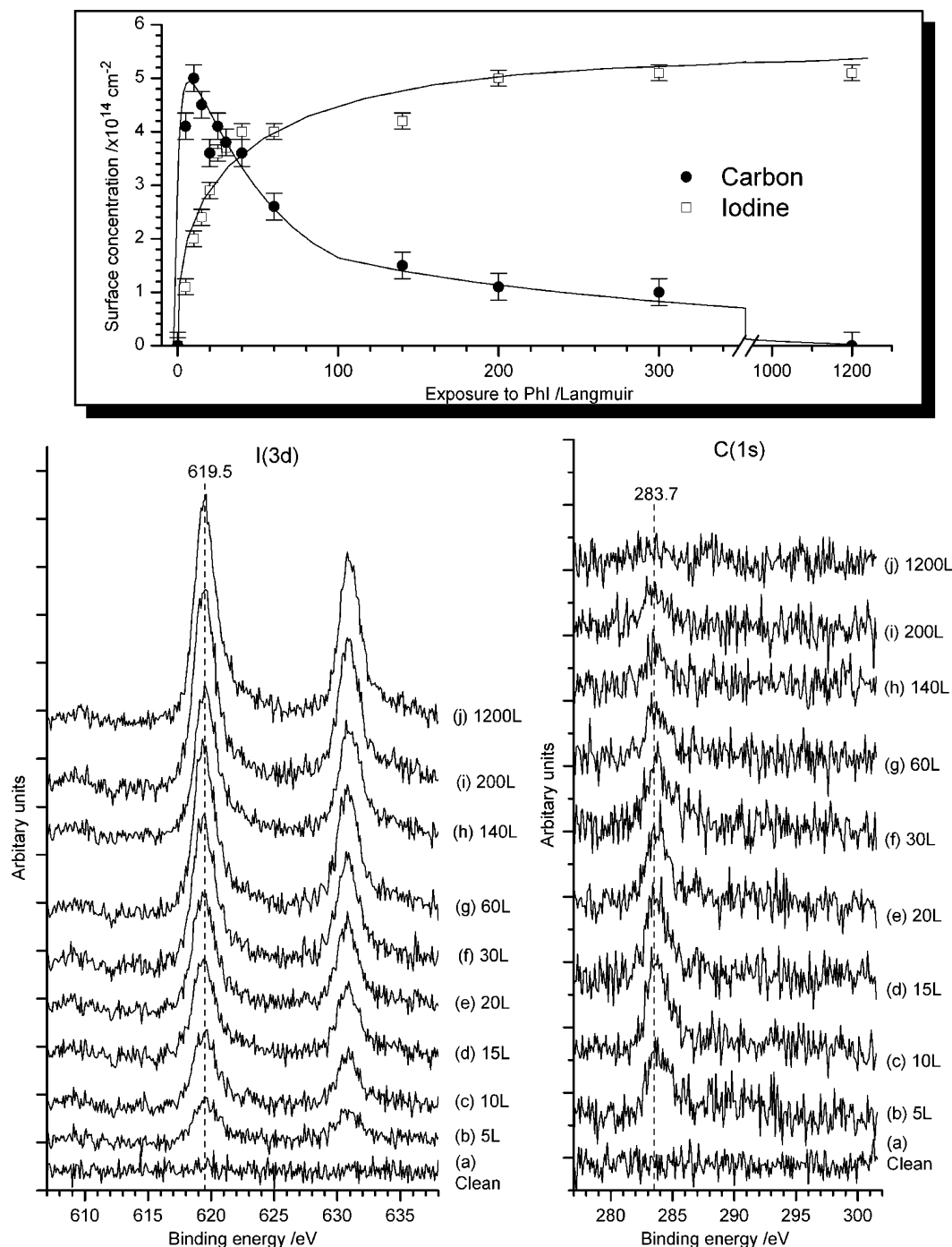


Figure 3. XP I(3d) and C(1s) spectra of the dissociative chemisorption of phenyl iodide at a clean Cu(110) surface at 290 K. Exposures to PhI are given on the figure. Inset: the surface concentration of iodine and carbon calculated from the XP spectra plotted as a function of exposure. The solid lines are to guide the eye.

$c(2 \times 2)$ I lattice are aligned (in the $\langle 1\bar{1}0 \rangle$ direction) with those of the $p(2 \times 1)\text{O(a)}$ lattice; this point will be considered in the discussion.

Phenyl Iodide Adsorption at Clean Cu(110) Surfaces. Figure 3 shows I(3d) and C(1s) spectra of a clean Cu(110) surface exposed to phenyl iodide at 290 K. After 5 L, an I(3d $_{5/2}$) peak is present at a binding energy of 619.5 eV, characteristic of chemisorbed iodine and hence dissociative adsorption of PhI. In contrast to MeI, a peak in the C(1s) spectrum indicates significant carbon adsorption with the comparatively low binding energy of 283.7 eV being typical of phenyl groups adsorbed at metal surfaces.^{13,20} Inset in Figure 3 is a plot of the variation of carbon and iodine surface concentrations with exposure to PhI.

Whereas the iodine concentration increases with exposure, reaching a maximum value of $5.5 \times 10^{14} \text{ cm}^{-2}$ after approximately 1200 L, the carbon concentration reaches a maximum of $5.1 \times 10^{14} \text{ cm}^{-2}$ after ca. 6 L but thereafter declines with exposure until, after 1200 L PhI, there is no longer evidence for carbon at the surface.

The STM images in Figure 4 show the development of the mixed phenyl/iodine adlayer with PhI exposure. At low exposures (≤ 50 L, Figure 4a) the iodine lattice is not atomically resolved, but discrete features are imaged at the top and bottom of some step edges after 10 L. These are convex in profile with a diameter of ~ 0.7 nm and a separation between features of approximately 1 nm. They are assigned to adsorbed phenyls.

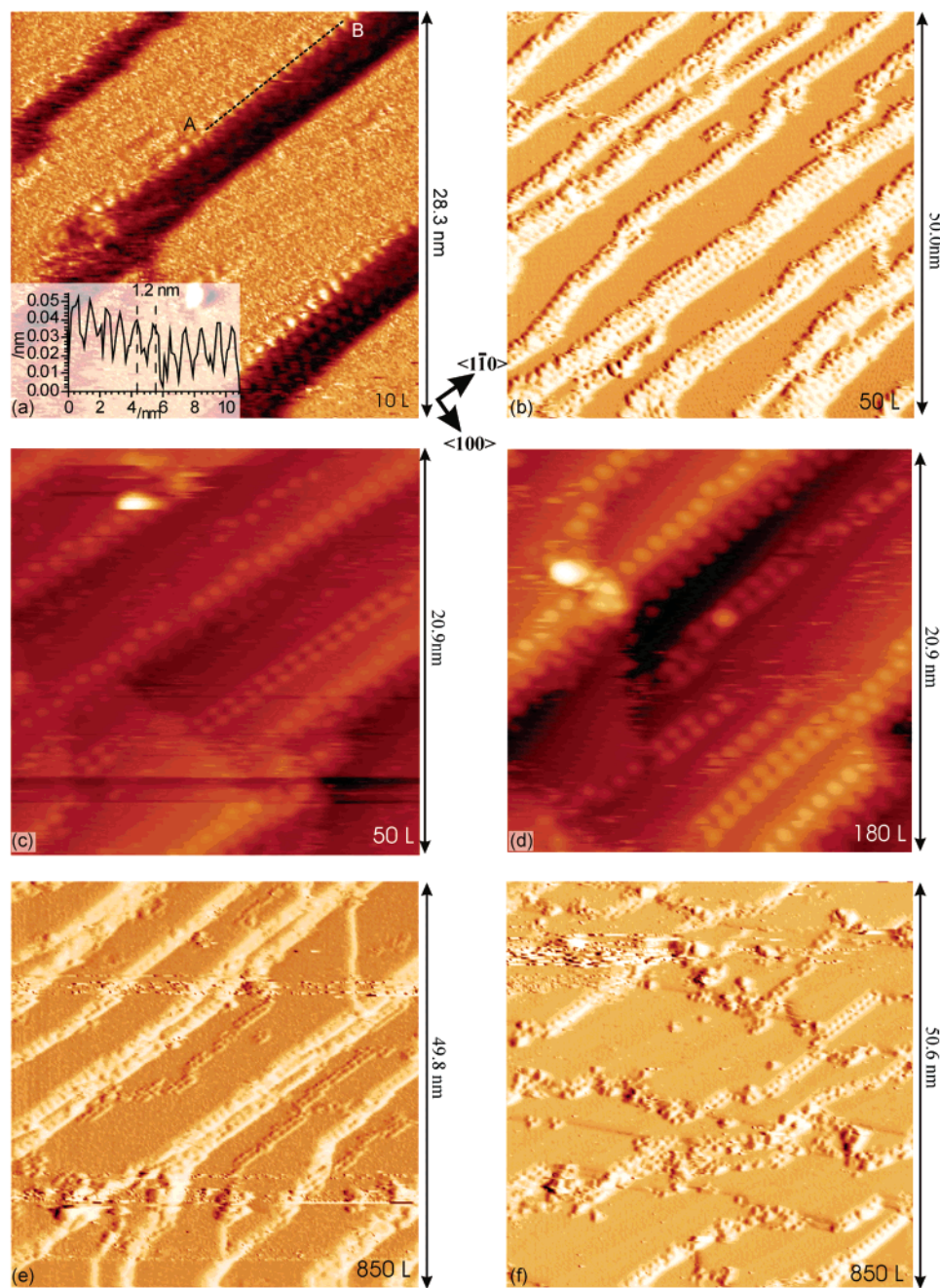


Figure 4. Development of the local surface structure at a Cu(110) surface as a function of exposure to PhI. STM images were recorded after successive exposures to PhI at 290 K. Exposures are given on the figure. (a) $V_S = 2.49$ V, $I_T = 2.40$ nA. Inset into (a) is the line profile along AB showing the regular 1 nm spacing between maxima in the $\langle 110 \rangle$ direction. (b–f) $V_S = -2.88$ V, $I_T = 1.42$ nA.

After 50 L most of the step edges are decorated with similar features (Figure 4b), and some are also present on the terraces, forming pairs of chains. The chains are separated by 1.0 nm in the $\langle 100 \rangle$ direction and extend up to 20 nm in the $\langle 110 \rangle$ direction, (Figure 4c). Some single $\langle 1\bar{1}0 \rangle$ orientated chains are also present but they are less common. Further exposure to PhI results in a surface with greater stability in which the bright features on the terraces and the $c(2 \times 2)$ lattice (assigned to I(a)) can be simultaneously imaged (Figures 4d–f and close-up in Figure 7a,b).

The relative stability of the phenyl groups in different adsorption sites can be deduced from Figure 5, which shows seven consecutive images recorded at 290 K from an area of the surface immediately after exposure to 180 L of phenyl iodide. Phenyls at step edges are immobile for all of the scans; those in paired chains are also stationary with the exception of

the molecules at the ends of the chains or in short lengths of paired chains which show a limited amount of movement between images. The phenyl groups incorporated into “unpaired” chains, however, are relatively unstable, showing substantial movement of groups of molecules occurring between consecutive scans

Higher exposures to PhI result in a reduction in the number of phenyl groups at the surface, in agreement with the XP results (Figure 3). However, somewhat surprisingly in light of the observations above on the stability of the different adsorption sites, the images do not show preferential removal of one type of phenyl over another with exposure; at 850 L for example, phenyl groups are present at both the step edges and on the terraces.

Figure 6 shows a closer study of the mixed phenyl/iodine adlayer present after an exposure of 180 L PhI. A typical single

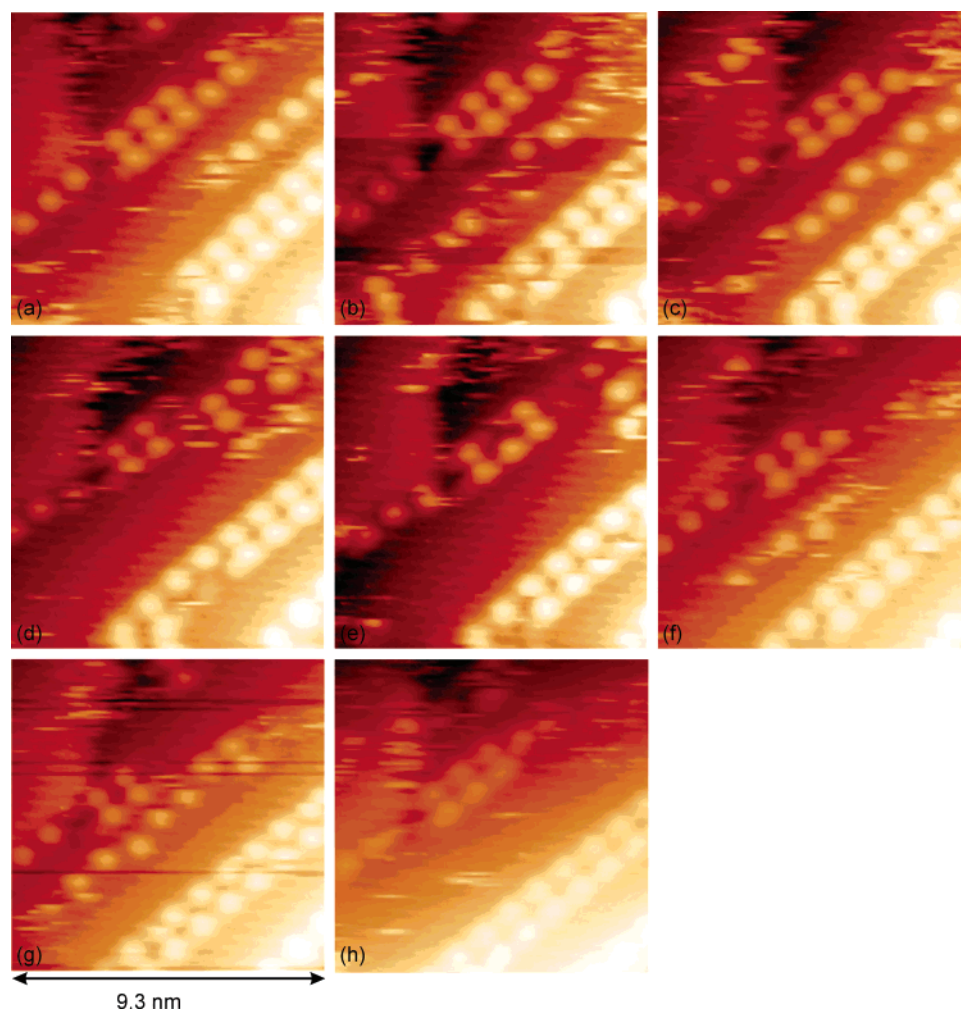


Figure 5. Sequence of STM images of the Cu(110) surface recorded after an exposure of 180 L PhI. The images show the rapid movement of the phenyl groups in unpaired chains and the relative stability of the paired chains (each image took 55 s to acquire). Note, however, that there is some movement of phenyl groups in the paired chains; mostly those at the ends of chains but also individual groups in the centers of the chains. Scanning conditions for all images were $V_s = -2.88$ V, $I_T = 1.42$ nA.

step with an apparent height of 0.12 ± 0.01 nm (unchanged from that of the clean surface) is shown in Figure 6a and in the expanded section (i). The $c(2 \times 2)I$ lattice is present on both the lower and upper terraces of the step. A paired chain of phenyl groups is located at the base of the step, and a profile over them (Profile 1, Figure 6b) shows the apparent height of the phenyl group to be almost equal to that of the step. Figure 6a also shows a set of bunched steps with a total apparent height difference between the upper and lower terraces of 0.34 nm, indicating three copper steps. In (ii), an expanded section of the image shows phenyl groups aligned along the top and bottom of the steps and also at two different apparent heights in the middle of the sequence, indicating two intermediate short terraces. A 3d version of (ii) is shown in (c) and a model of the structure of the step is given in (d). Apparent height changes along the lines 2 and 3 are plotted in profiles 2 and 3 in Figure 6b; these are considered, together with the models in Figure 6e,f, in the discussion.

Finally, the simultaneous imaging of the phenyl groups and the $c(2 \times 2)I(a)$ lattice in Figure 7a allows a comparison of the two structures. Extrapolating the iodine lattice over the phenyl chains we find that the centers of the phenyl groups are situated in equivalent sites to the iodine adatoms. We also note that the maxima in the $c(2 \times 2)I(a)$ lattice either side of the phenyl group chains are often not aligned; evidently the phenyl groups are adsorbed in a grain boundary between iodine islands.

Adsorption of Phenyl Iodide in the Presence of Chemisorbed Oxygen. When partially oxidized Cu(110) surfaces are exposed to phenyl iodide at 290 K, XP spectra show dissociative adsorption and the presence of chemisorbed phenyl groups at low exposures, which are removed at higher exposures or by heating. The final concentration of iodine is limited by the presence of the oxygen, so that at saturation $\sigma_O + \sigma_I = 5.5 \times 10^{14}$ atoms cm^{-2} . The C(1s) and I(3d) binding energies of the adsorbed phenyls and iodine are identical to those recorded after phenyl adsorption at the clean surface. However, the STM images recorded for these experiments are markedly different from those at the clean surface. Figure 8a was recorded after a surface with an initial oxygen concentration of 1.1×10^{14} cm^{-2} was exposed to 200 L of phenyl iodide at 290 K. The images show the phenyl groups clustered around the perimeters of the oxygen islands; there is almost no phenyl adsorption at the step edges. Clearly oxygen is not simply blocking adsorption sites. Figure 8b shows the surface after heating the sample to 400 K and subsequently cooling to room temperature; few phenyl groups are now observed in the STM images, and the surface is covered by oxygen and iodine. The latter is well resolved in the $\langle 100 \rangle$ direction but not in the $\langle 1\bar{1}0 \rangle$ direction, a characteristic feature of I(a) at the Cu(110) surface at concentrations less than saturation. Figure 8c shows the surface after heating to 500 K; no phenyl groups are now evident in the STM images and this is confirmed by the XPS data.

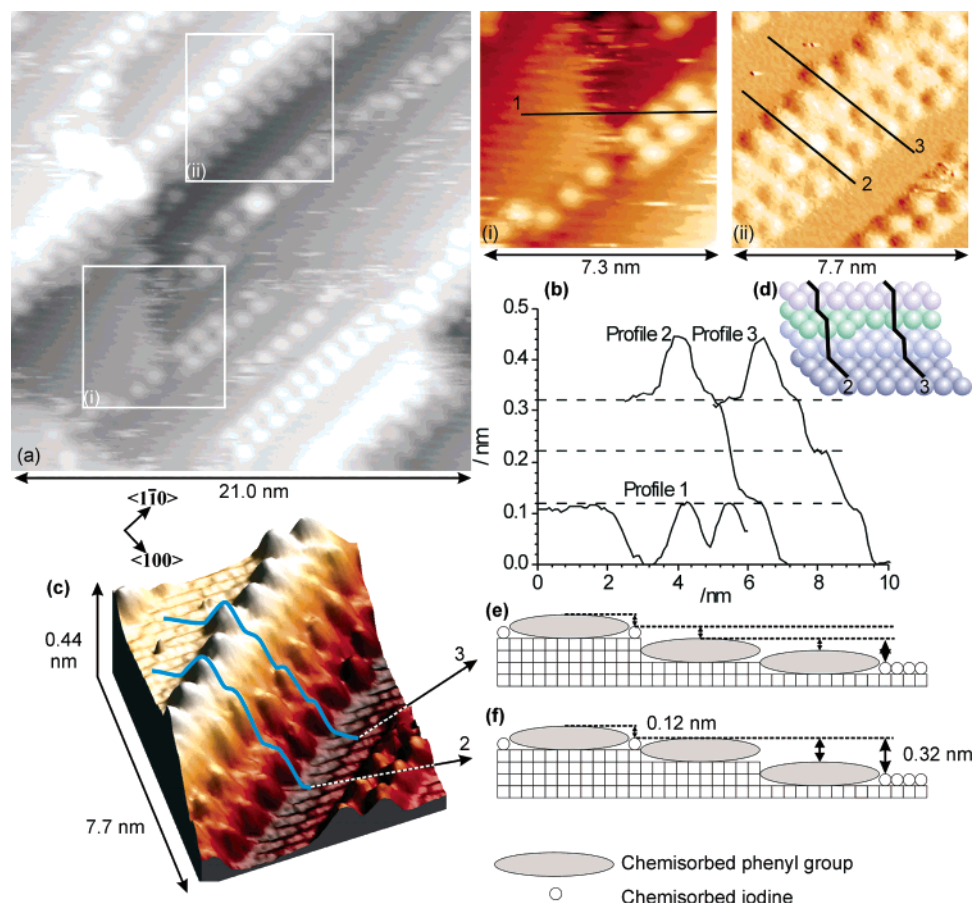


Figure 6. Analysis of the local structure of the phenyl groups at the Cu(110) surface. (a) STM image from Figure 4d recorded after an exposure of 180 L PhI; expanded sections of this image are shown in (i), which compares the apparent height of an adsorbed phenyl group with the apparent height of a single atomic step at the surface (profile 1), and in (ii), which shows phenyl groups adsorbed at a sequence of steps (profiles 2 and 3). Line profiles 1, 2, and 3 over the steps are shown in (b), and a 3D representation of the image in (ii) is shown in (c) and modeled in (d). (e) and (f) show schematic models of the apparent height differences observed in profiles 2 and 3, with the apparent height and width of the phenyl groups shown to scale.

Methyl and Phenyl Iodide Adsorption at Ag(111) Surfaces.

Exposure of the Ag(111) surface to methyl iodide at 290 K results in I(3d) peaks in the XP spectrum (not shown) at 619.0 and 630.4 eV, indicating iodine adsorption, but there is no evidence for the presence of carbon at the surface. The iodine peak binding energies are ~ 0.5 eV lower than those observed at the Cu(110) surface, but the absence of carbon clearly indicates dissociative adsorption of MeI, the formation of a chemisorbed iodine, and the desorption of the methyl groups. The iodine surface concentration (calculated from the XP peak areas) reaches a maximum of $4.6 \times 10^{14} \text{ cm}^{-2}$ corresponding to one-third of the number of silver atoms in the Ag(111) monolayer ($1.39 \times 10^{15} \text{ cm}^{-2}$) after an exposure of ~ 500 L, Figure 9 (inset).

Exposure of an Ag(111) surface to phenyl iodide at 290 K does result in some carbon adsorption, with the XP spectra showing a peak centered at a binding energy of 284.4 eV, Figure 9. The carbon concentration reaches a maximum of $1.1 \times 10^{14} \text{ cm}^{-2}$ after 50 L exposure to PhI but is reduced following further exposures and completely removed after 1000 L. The iodine peaks are at binding energies similar to those obtained after exposure of the silver surface to methyl iodide, suggesting dissociative adsorption, and the iodine concentration reaches a maximum of $4.5 \times 10^{14} \text{ cm}^{-2}$ after ~ 1000 L. Figure 9 (inset) plots the iodine concentration at the Ag(111) surface at 290 K as a function of exposure to MeI and PhI.

In the STM images, the clean Ag(111) surface (not shown) is characterized by large terraces ca. 20–30 nm in width

separated by single steps 0.23 nm in height. The step edges are characteristically “rough” at 290 K, indicating significant atom mobility at the steps.²¹ During exposure to methyl and phenyl iodide at 290 K the extent of step movement is increased with several short steps vanishing, but there is no evidence for atomically resolved ordered structures on the terraces until the iodine concentration approaches saturation. Figure 10a,b shows the atomically resolved ($\sqrt{3} \times \sqrt{3}$)R30 iodine adlayer formed after exposure to 500 L of PhI, with profiles across the surface shown in Figure 10c,d. The iodine lattice is well resolved, but there is no evidence in the images for the presence of phenyl groups. Figure 10e,f shows an example of a screw dislocation which is commonly observed at the Ag(111) surface, with the iodine adlayer clearly resolved on the terraces around the developing step.

Discussion

Quantification of the $\text{C}_6\text{H}_5(\text{a})$ and $\text{CH}_3(\text{a})$ Adsorbates at Cu(110) and Ag(111) Surfaces. The principal aims of this study were to determine the extent to which the methyl and phenyl groups formed from the dissociative adsorption of the alkyl halides adsorbed as stable species at Cu(110) and Ag(111) surfaces at 290 K; to characterize their adsorbed states; and to investigate the influence of iodine and oxygen coadsorbates on the adsorbed alkyl groups. The XPS data show dissociative adsorption in all cases and the desorption of the methyl groups formed from MeI, implying that previous studies based on TPD

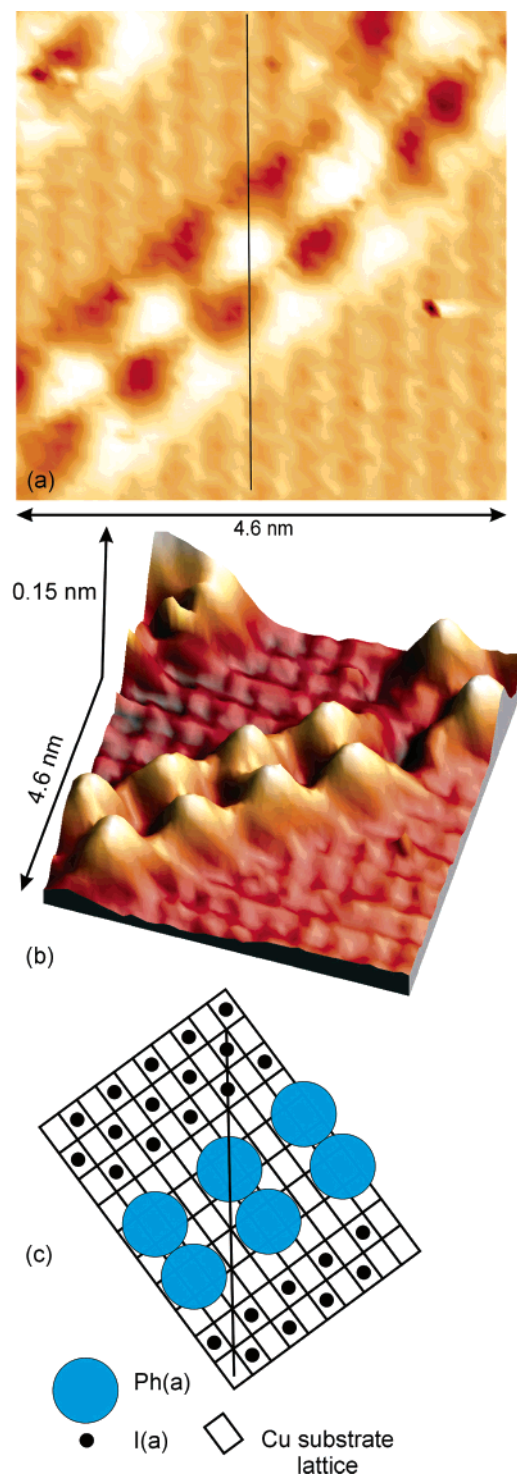


Figure 7. STM images showing coexisting $c(2 \times 2)$ I(a) and phenyl adsorbates at a Cu(110) surface. (a) After 180 L PhI, $V_s = -2.88$ V, $I_T = 1.41$ nA; note the offset between the maxima in the iodine lattice either side of the phenyl chain showing that the phenyl groups are situated in a grain boundary in the iodine lattice. (b) 3D representation of (a) showing clearly the I(a) maxima. (c) Schematic model of the coexisting iodine and phenyl lattices.

and vibrational techniques,^{1,11} which have reported methyl desorption above room temperature relate to methyl concentrations that are below the XPS detection limit ($\sim 5 \times 10^{13} \text{ cm}^{-2}$). On the other hand, the XPS and STM data show that chemisorbed phenyls are stable at the copper surface after intermediate exposures to PhI and possibly at the Ag(111) surface. The relatively low C(1s) binding energy associated with these

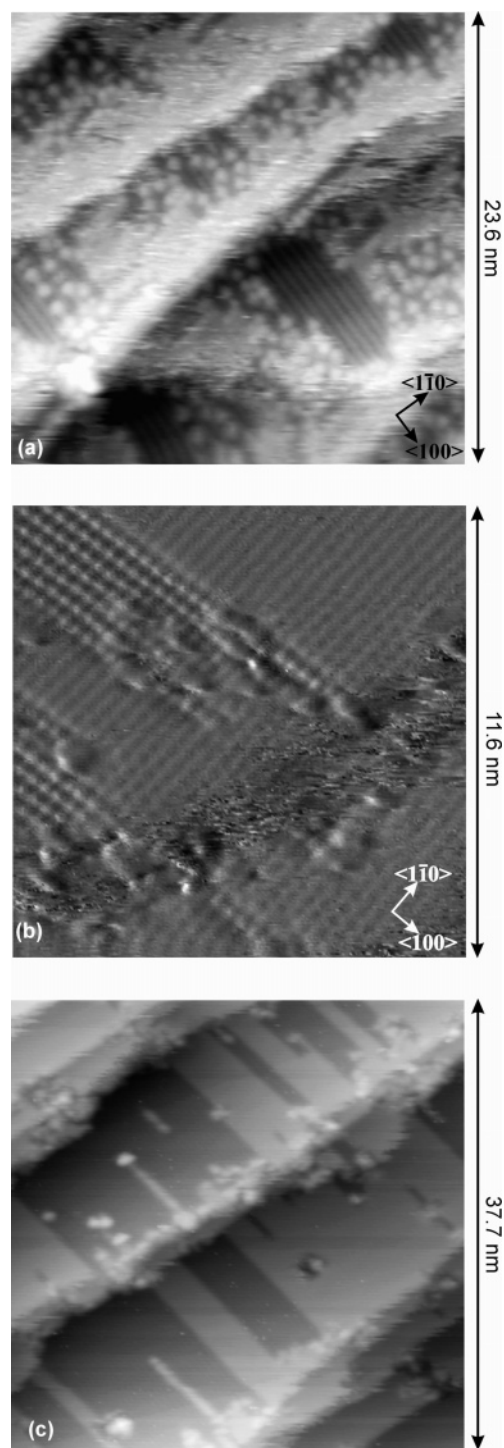


Figure 8. STM images of a partially oxidized Cu(110) surface, $\sigma_0 = 1.1 \times 10^{14} \text{ cm}^{-2}$ exposed to 40 L PhI, $\sigma_1 = 1.3 \times 10^{14} \text{ cm}^{-2}$. (a) Image showing the clustering of phenyl groups at the perimeters of the $p(2 \times 1)$ O(a) islands; note the absence of the <110> orientated phenyl chains which characterized phenyl adsorption at the clean Cu(110) surface either at the step edges or on the terraces. $V_s = -0.88$ V, $I_T = 3.60$ nA. (b) After warming surface (a) to 400 K for 30 min, $V_s = 0.95$ V, $I_T = 1.90$ nA. (c) After warming surface (b) to 500 K for 30 min, $V_s = 0.95$ V, $I_T = 1.93$ nA.

adsorbates reflects the high electron density of the ring and is similar to values reported for phenyl containing groups at other metal surfaces.^{13,22} The XPS data allow us to follow the surface composition quantitatively as a function of phenyl iodide exposure. At the Cu(110) surface the iodine concentration increases steadily with exposure, whereas the phenyl group

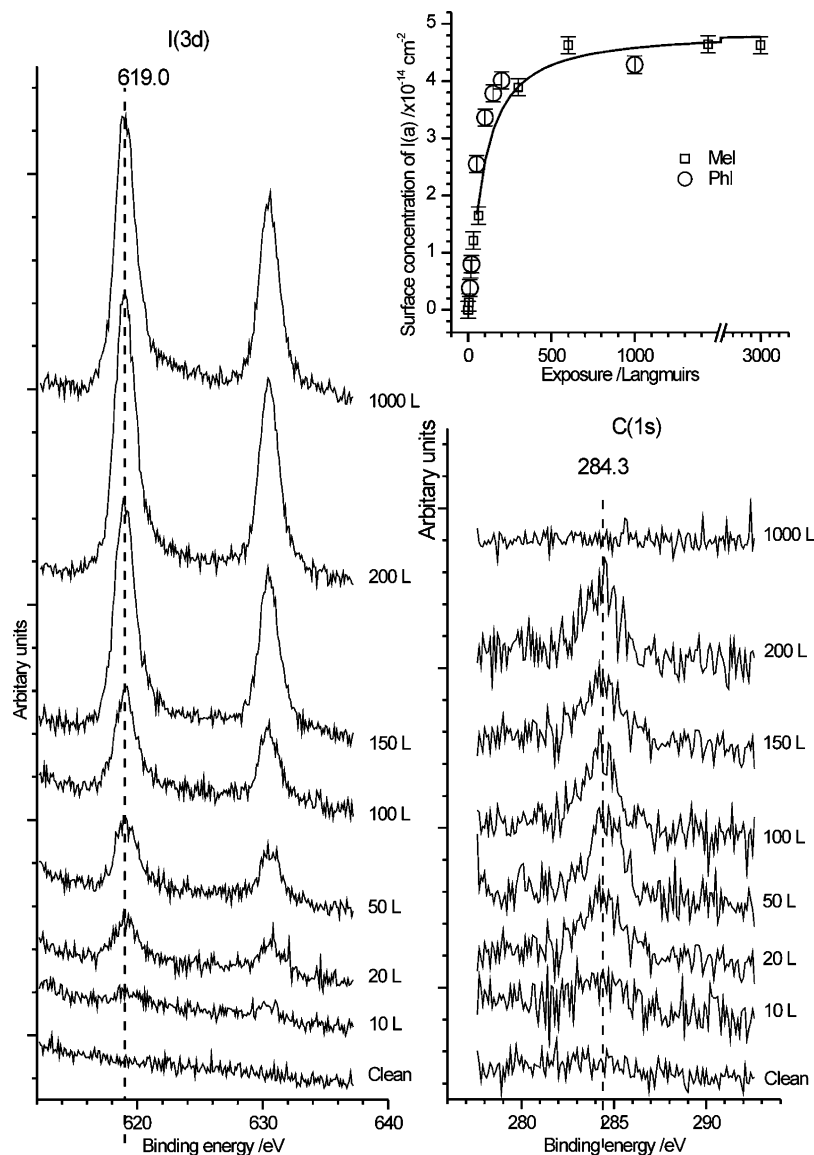


Figure 9. XP I(3d) and C(1s) spectra of the dissociative chemisorption of phenyl iodide at a clean Ag(111) surface at 290 K. Exposures to PhI are given on the figure. Inset: comparison of the surface concentration of iodine as a function of exposure to MeI and PhI. The solid line is to guide the eye.

concentration reaches a maximum after ~ 6 L and thereafter decreases with exposure. This observation is consistent with the coupling of phenyl groups and the subsequent desorption of biphenyl; biphenyl desorption was reported⁶ at 400 K following the adsorption of phenyl iodide at Cu(111) surfaces at low temperatures. The 6:1 C/I ratio observed at low PhI exposures suggests biphenyl formation is unfavorable compared to phenyl chemisorption but, as the coverage increases, desorption becomes the favored pathway presumably because of a lack of adsorption sites. Very high exposures of PhI (~ 1000 L) result in the removal of all the phenyl groups from the surface.

The STM images show the Cu(110) surface to be saturated with a mixed iodine/phenyl adlayer after ~ 6 L exposure to PhI, and further adsorption of iodine can take place only if accompanied by the desorption of a phenyl group. Assuming a simple chessboard model of the system with the phenyl adsorption directly at the copper surface and not over the iodine adatoms, the number of sites available for iodine adsorption is limited to the total number of sites minus those already occupied by iodine or blocked by adsorbed phenyls. Taking the saturation concentration of iodine as $5.5 \times 10^{14} \text{ cm}^{-2}$, the data in Figure 3 can be fitted with this model if a phenyl group blocks between

3.5 and 4 iodine adsorption sites, consistent with the observed 7 nm diameter of the phenyl group (Figures 6e,f and 7c).

Structure of the Iodine Adlayer. Figure 2 establishes that iodine forms a $c(2 \times 2)$ structure at the Cu(110) surface consistent with the saturation iodine concentration of $5.5 \times 10^{14} \text{ cm}^{-2}$ calculated from the XP spectra, and also with the structures previously reported for chlorine and bromine at Cu(110) surfaces.²³ At concentrations below a monolayer, and in the absence of other site blocking adsorbates, iodine does not form islands as sulfur¹⁸ does, for example. Instead, a structure consisting of $\langle 1\bar{1}0 \rangle$ aligned rows that could not be atomically resolved is observed. Poor resolution in STM images is often associated with mobility, and we interpret the present results as indicating relatively facile diffusion of iodine in the $\langle 110 \rangle$ direction and a much lower rate of diffusion in the $\langle 100 \rangle$ direction.

Where oxygen and iodine are simultaneously present separate phases are formed, Figure 2c. The oxygen adlayer consists of added Cu–O rows orientated in the $\langle 100 \rangle$ direction, with the oxygen situated in the short bridge sites of the unreconstructed surface and the added row copper in the hollow sites.^{24–26} It has been established²⁷ that under normal imaging conditions

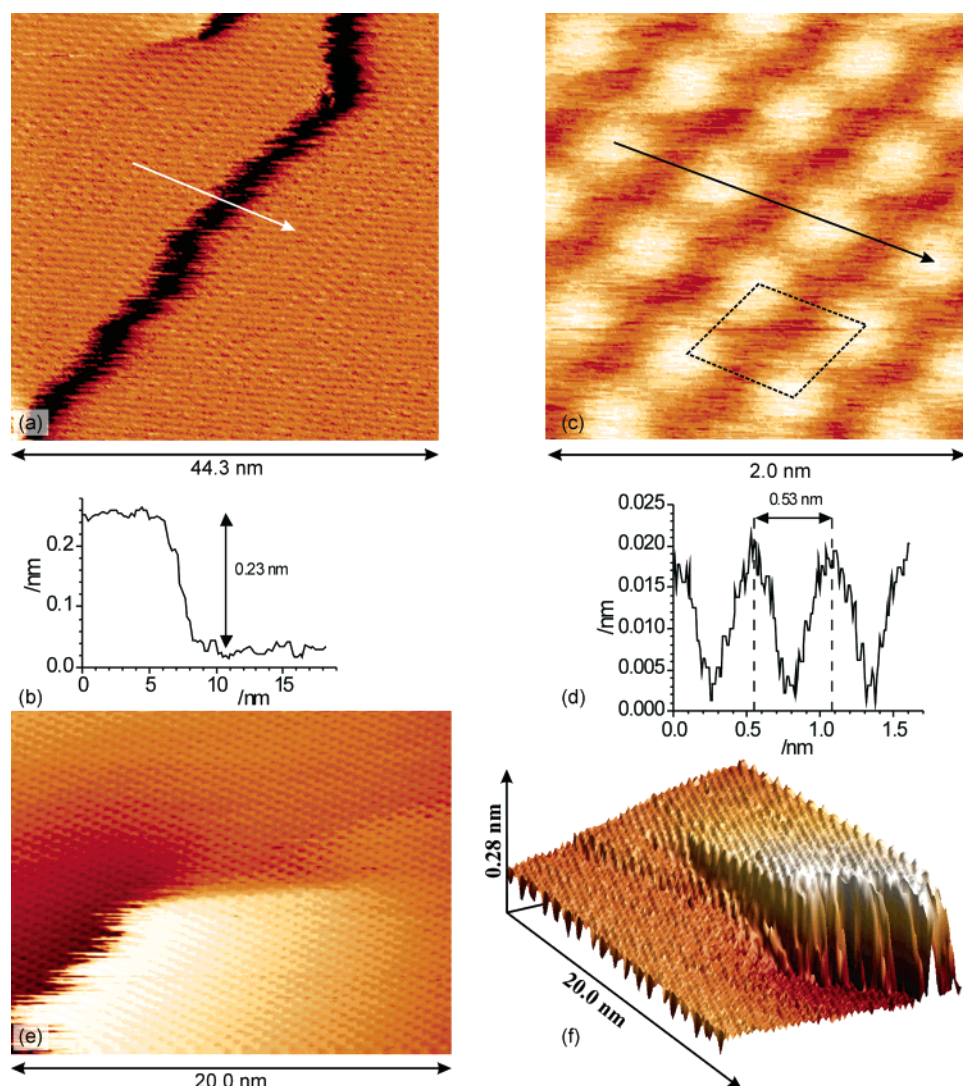


Figure 10. STM images of the iodine adlayer formed at a Ag(111) surface by the dissociative adsorption of phenyl iodide at 290 K. (a) After exposure to 500 L PhI, $\sigma_I = 5.5 \times 10^{14} \text{ cm}^{-2}$, $V_S = -0.02 \text{ V}$, $I_T = 2.89 \text{ nA}$. Note apparent step height in line profile (b) is similar to that of clean Ag(111). (c) Close-up of I(a) unit cell, $V_S = 0.02 \text{ V}$, $I_T = 2.50 \text{ nA}$. (d) line profile from (c). (e, f) Showing continuous iodine lattice around a screw dislocation at the surface, $V_S = 0.99 \text{ V}$, $I_T = 2.12 \text{ nA}$.

the copper adatoms are imaged as maxima by STM, therefore the extrapolation of the $p(2 \times 1)\text{O(a)}$ structure over the iodine lattice in Figure 2 provides good evidence that the maxima in the iodine lattice are situated in the same adsorption sites as the added copper. We conclude that iodine adsorbs near the 2-fold hollow site of the Cu(110) surface with a low activation energy for diffusion along the $\langle 1\bar{1}0 \rangle$ direction and a somewhat higher barrier to diffusion in the $\langle 100 \rangle$ direction. This conclusion is in agreement with the finding by Pascal et al.²⁸ that iodine adsorbs in the hollow sites at Cu(111) surfaces.

At the Ag(111) surface, chemisorbed iodine forms a hexagonal lattice with a 0.53 nm primitive unit cell identical to that expected for a $(\sqrt{3} \times \sqrt{3})R30^\circ$ structure. There is no readily available reference structure in our data with which to compare the iodine adlayer, and therefore the adsorption site cannot be probed in any more detail. Interestingly, no features were observed in the STM images that could be assigned to the phenyl groups at the Ag(111) surface after exposure to PhI, despite the XP data indicating the presence of a carbon-containing species. Possibly the phenyl groups adsorb close to step edges where the STM tip has difficulty resolving them, or else they are too weakly bound (and therefore too mobile) to be imaged by the STM tip.

Chemisorbed Phenyl Groups. The $\text{I}(3d^{5/2})$ XP peak at 619.5 eV on Cu(110) is characteristic of chemisorbed iodine, indicating that the phenyl iodide dissociates at the Cu(110) surface at 290 K. On the basis of their dependence on exposure to PhI, the bright 0.7 nm diameter features in the STM images can be assigned to chemisorbed phenyl groups. These are mostly present as chains orientated in the $\langle 1\bar{1}0 \rangle$ direction and adsorbed either singly at step edges or as pairs on the terraces, with occasional single chains also imaged on the terraces. The latter are clearly unstable at 290 K, with groups of more than 7 molecules jumping position in the space of a single STM image (see for example Figure 5).

Figure 6 gives a more detailed insight into the apparent height of the adsorbates. Profile 1 shows the chemisorbed phenyl rings to be $0.11 \pm 0.01 \text{ nm}$ above the iodine lattice; we discussed above how both the STM data and the XPS data suggest that the phenyls adsorb directly at the copper surface between iodine islands. Profiles 2 and 3 show height profiles over a sequence of steps. The models in Figure 6d,e show the relative heights of the phenyl and iodine adsorbates at the multiple step sites, with the diameter of the phenyl rings drawn in proportion to the apparent height. From these models, an apparent height of the chemisorbed iodine above the copper surface of 0.1 nm is

established, and hence the apparent height of the phenyl group above the copper is 0.21 ± 0.01 nm.

Comparison between iodine and phenyl adsorbates also provides information on the adsorption site of the phenyl rings; Figure 7a shows the centers of the phenyl groups aligned with the maxima in one of the I(a) islands. It was established above that iodine adatoms adsorb preferentially in the two-fold hollow sites at the Cu(110) surface. Figure 7a therefore suggests that the phenyl group adsorption site is centered at either the hollow or atop sites (see model in Figure 7c). Recent studies²⁰ of phenyl imides at Cu(110) surfaces show adsorption of the phenyl ring at a hollow site, and calculations²⁹ have indicated that benzene adsorbs 0.2 nm above hollow sites at Cu(110) surfaces. On the other hand a low-temperature STM study³⁰ suggested benzene adsorption favored the long bridge site.

The perimeters of the $p(2 \times 1)O(a)$ islands at the Cu(110) surface clearly provide highly stable sites for the phenyl groups which dominate over even the stable sites at step edges. However, the XPS shows no change in the binding energies of either the carbons in the phenyl ring or the chemisorbed oxygen. On heating, the stabilized phenyls desorb, presumably as biphenyls; our temperature measurement is not sufficiently precise to determine whether the oxygen has a stabilizing effect on the adsorbed species.

Conclusions

The chemisorption of phenyl iodide and methyl iodide has been studied at Cu(110) and Ag(111) surfaces at 290 K. Dissociation of both molecules leads to chemisorbed iodine at both surfaces, but methyl groups are not stable and desorb immediately, presumably as ethane. Phenyl groups are present at the Cu(110) surface after phenyl iodide dissociation, and the mixed phenyl $c(2 \times 2)I(a)$ adlayer has been imaged by STM and characterized by XPS. The phenyl rings are stabilized at the top and bottom of step edges and on the terraces through the formation of chains, often paired, which are orientated in the $\langle 110 \rangle$ direction. Isolated phenyl groups are also present on the terraces but are relatively mobile at room temperature. XP data establish that each ring blocks approximately 4 iodine adsorption sites, and a comparison of the phenyl structure with the coadsorbed iodide adlayer in the STM images shows that the rings adsorb preferentially in hollow or atop sites with the ring plane close to horizontal. At the Ag(111) surface there is evidence from XPS for the presence of chemisorbed phenyl groups, but they are not imaged by STM. The iodine adlayer forms a $(\sqrt{3} \times \sqrt{3})R30^\circ$ structure at the Ag(111) surface.

Acknowledgment. The authors acknowledge stimulating discussions with Prof. M. W. Roberts and, in addition, M.C. and D.J.M. gratefully acknowledge support from CBDE, Porton Down, UK, and Magnox Electric. This work was also supported by EPSRC.

References and Notes

- (1) Bent, B. E. *Chem. Rev.* **1996**, 96, 1361.
- (2) Xi, M.; Bent, B. E. *J. Am. Chem. Soc.* **1993**, 115, 7426.
- (3) Bent, B. E.; Nuzzo, R. G.; Zegarski, B. R.; Dubois, L. H. *J. Am. Chem. Soc.* **1991**, 113, 1143.
- (4) Chiang, C. M.; Wentzlaff, T. H.; Bent, B. E. *J. Phys. Chem.* **1992**, 96, 1836.
- (5) Chiang, C. M.; Bent, B. E. *Surf. Sci.* **1992**, 279, 79.
- (6) Xi, M.; Bent, B. E. *Surf. Sci.* **1992**, 278, 19.
- (7) Kash, P. W.; Sun, D. H.; Xi, M.; Flynn, G. W.; Bent, B. E. *J. Phys. Chem.* **1996**, 100, 16621.
- (8) Yang, M. X.; Xi, M.; Yuan, H. J.; Bent, B. E.; Stevens, P.; White, J. M. *Surf. Sci.* **1995**, 341, 9.
- (9) Jenks, C. J.; Paul, A.; Smoliar, L. A.; Bent, B. E. *J. Phys. Chem.* **1994**, 98, 572.
- (10) Jenks, C. J.; Bent, B. E.; Bernstein, N.; Zaera, F. *J. Phys. Chem. B* **2000**, 104, 3008.
- (11) Jenks, C. J.; Bent, B. E.; Zaera, F. *J. Phys. Chem. B* **2000**, 104, 3017.
- (12) Whelan, C. M.; Cecchet, F.; Baxter, R.; Zerbetto, F.; Clarkson, G. J.; Leigh, D. A.; Rudolf, P. *J. Phys. Chem. B* **2002**, 106, 8739.
- (13) Cabibil, H.; Ihm, H.; White, J. M. *Surf. Sci.* **2000**, 447, 91.
- (14) Yang, M. X.; Jo, S. K.; Paul, A.; Avila, L.; Bent, B. E.; Nishikida, K. *Surf. Sci.* **1995**, 325, 102.
- (15) Paul, A. M.; Bent, B. E. *J. Catal.* **1994**, 147, 264.
- (16) Sung, D.; Gellman, A. J. *Surf. Sci.* **2004**, 551, 59.
- (17) Carley, A. F.; Roberts, M. W. *Proc. R. Soc. London, Ser. A* **1978**, 363, 403.
- (18) Carley, A. F.; Davies, P. R.; Jones, R. V.; Harikumar, K. R.; Kulkarni, G. U.; Roberts, M. W. *Surf. Sci.* **2000**, 447, 39.
- (19) WSxM. <http://www.nanotec.es>.
- (20) Davies, P. R.; Edwards, D.; Richards, D. *J. Phys. Chem. B* **2004**, 108, 18630.
- (21) Quaas, N.; Wenderoth, M.; Ulbrich, R. G. *Surf. Sci.* **2004**, 550, 57.
- (22) Carley, A. F.; Coughlin, M.; Davies, P. R.; Morgan, D. J.; Roberts, M. W. *Surf. Sci.* **2004**, 555, L138.
- (23) Carley, A. F.; Davies, P. R.; Harikumar, K. R.; Jones, R. V.; Roberts, M. W., in preparation.
- (24) Kuk, Y.; Chua, F. M.; Silverman, P. J.; Meyer, J. A. *Phys. Rev. B, Condens. Matter* **1990**, 41, 12393.
- (25) Jensen, F.; Besenbacher, F.; Laesgaard, E.; Stensgaard, I. *Phys. Rev. B* **1990**, 41, 10233.
- (26) Coulman, D. J.; Wintterlin, J.; Behm, R. J.; Ertl, G. *Phys. Rev. Lett.* **1990**, 64, 1761.
- (27) Doering, M.; Buisset, J.; Rust, H. P.; Briner, B. G.; Bradshaw, A. M. *Faraday Discuss.* **1996**, 163.
- (28) Pascal, M.; Lamont, C. L. A.; Kittel, M.; Hoeft, J. T.; Constant, L.; Polcik, M.; Bradshaw, A. M.; Toomes, R. L.; Woodruff, D. P. *Surf. Sci.* **2002**, 512, 173.
- (29) Rogers, B. L.; Shapter, J. G.; Ford, M. *Surf. Sci.* **2004**, 548, 29.
- (30) Doering, M.; Rust, H. P.; Briner, B. G.; Bradshaw, A. M. *Surf. Sci.* **1998**, 410, L736.